

Transport modeling applied to the interpretation of groundwater ^{36}Cl age

Jungho Park and Craig M. Bethke

Department of Geology, University of Illinois, Urbana, Illinois, USA

Thomas Torgersen

Department of Marine Science, University of Connecticut, Groton, Connecticut, USA

Thomas M. Johnson

Department of Geology, University of Illinois, Urbana, Illinois, USA

Received 13 February 2001; revised 9 November 2001; accepted 9 November 2001; published 3 May 2002.

[1] We use reactive transport modeling to consider how diffusion and hydrodynamic dispersion, cross-formational flow, and subsurface production affect the steady state distribution in flow regimes of the radioactive isotope ^{36}Cl , and the relationship of the isotope distribution to groundwater residence time, or “age.” The isotope forms naturally in the atmosphere, dissolves in rainwater, and then decays in the subsurface with a half-life of $\sim 301,000$ years; hence it is important for age dating very old groundwater. In a simple flow regime composed of an aquifer confined above and below by aquitards, isotopic age may correspond rather well with a groundwater’s “piston flow” age. This correspondence is favored where the aquifer is thick, cross-formational flow is insignificant, salinity is low, and the diffusion coefficient within the aquitards is small. The maximum dateable age, however, is somewhat smaller than expected from the isotope’s half-life. Owing to the effect of “dead” chloride, dating based on isotope abundance (the $^{36}\text{Cl}/\text{Cl}$ ratio) may be less accurate than that based on ^{36}Cl concentration. Cross-formational flow can strongly affect the ^{36}Cl distribution and abundance, preventing the rates and even direction of flow within an aquifer from being interpreted using the piston flow model. Where salinity is moderate or high, the isotope distribution is controlled by subsurface production, and dating on the basis of the decay of atmospheric ^{36}Cl is not possible. In models of simple flow regimes the ^{36}Cl method fails to predict groundwater age accurately where groundwater chlorinity exceeds $\sim 75\text{--}150\text{ mg kg}^{-1}$. Reactive transport models hold considerable promise for improving interpretation of the rates and patterns of groundwater flow from radioisotope distributions. **INDEX TERMS:** 1035 Geochemistry: Geochronology; 1040 Geochemistry: Isotopic composition/chemistry; 1829 Hydrology: Groundwater hydrology; 1832 Hydrology: Groundwater transport; 3210 Mathematical Geophysics: Modeling; **KEYWORDS:** chlorine 36, groundwater age, groundwater modeling, diffusion

1. Introduction

[2] One of the most fundamental tasks in the study of a groundwater flow regime is determining how the residence time (or “age”) of the groundwater varies across the system. Most commonly, we use Darcy’s law to calculate flow velocity, the knowledge of which lets us compute groundwater age. Darcy’s law requires as input the distribution within the domain of hydraulic conductivity, hydraulic gradient, and porosity. None of these values can be known exactly; especially, appropriate values for hydraulic conductivity can be difficult to constrain. Hence characterizing a flow regime using Darcy’s law carries a certain level of inherent uncertainty.

[3] Groundwater age can also be computed directly by observing the distribution of an isotope that decays in the subsurface or is produced there at a predictable rate; the velocity field can then be calculated from variation in age with distance. A number of radiogenic and radioactive isotopes, most notably ^{14}C , have been used for this purpose [e.g., Fröhlich *et al.*, 1991; Lehmann *et al.*, 1993]. Residence time determined by isotopic methods can provide

an alternative means of characterizing a flow system or serve as a check on the results of applying Darcy’s law.

[4] In the study of very old groundwater, such as that found in regional flow regimes or deep in the Earth’s crust, isotopic methods can be especially important because reliable information about the distribution of hydraulic conductivity in such environments is commonly difficult to obtain. To be useful in dating very old groundwater, an isotope must decay or be produced quite slowly and be little affected by chemical reaction. The noble gas isotopes ^4He and ^{40}Ar , which are derived in the subsurface from the radioactive decay chains of U, Th, and K, meet these requirements, as does ^{36}Cl , which is produced naturally in the atmosphere and decays in groundwater [Lehmann *et al.*, 1993; Bethke *et al.*, 1999b].

[5] The ^{36}Cl method is attractive for dating very old groundwater because of the isotope’s long half-life ($T_{1/2}$) of $\sim 301,000$ (± 4000) year [Bentley *et al.*, 1986a], which allows dating of samples with ages ranging from $\sim 10^5$ to 10^6 year. In addition, because of its high electronegativity, chlorine most commonly occurs in the subsurface as the free chloride ion. Hence the distribution of ^{36}Cl should be little affected by chemical interaction with the host rock [Bentley *et al.*, 1986a; Seaman *et al.*, 1996]. The

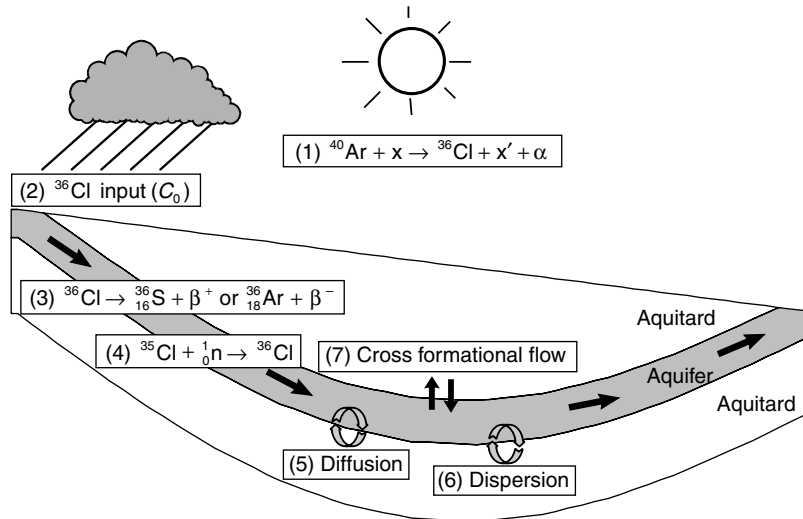
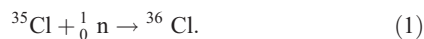


Figure 1. Some factors affecting the distribution ^{36}Cl in a regional groundwater flow regime. Chlorine 36 is produced in the atmosphere (1) and dissolves in rainwater. Rainwater infiltrates the subsurface (2) and may be concentrated by evapotranspiration in the soil zone; the initial ^{36}Cl concentration is C_0 . As groundwater migrates along an aquifer, the radioactive ^{36}Cl decays (3). Chlorine 36 is produced in situ by neutron activation of the stable isotope ^{35}Cl (4); the subsurface production rate is proportional to groundwater chlorinity and the neutron flux resulting from the alpha decay chains of U and Th. Chlorine 36 may be lost from the aquifer by diffusion into aquitards containing little of the isotope or gained by diffusion from areas where the rate of subsurface production is great (5). Mixing between aquifer and aquitards by hydrodynamic dispersion may increase or decrease the ^{36}Cl concentration (6). Cross-formational flow carries ^{36}Cl into and out of aquifer (7).

method has been applied to study groundwater flow in, for example, the Great Artesian Basin of Australia [Bentley *et al.*, 1986b; Torgersen *et al.*, 1991; Love *et al.*, 2000], the Milk River aquifer of the Western Canada Sedimentary Basin [Phillips *et al.*, 1986; Nolte *et al.*, 1991], and the Aquia aquifer in the Maryland coastal plain [Purdy *et al.*, 1996].

[6] There are, nonetheless, significant uncertainties associated with applying the method. The concentration of ^{36}Cl at recharge can vary with climatic conditions, as can the isotope's abundance (the mole ratio $^{36}\text{Cl}/\text{Cl}$). Previous studies [e.g., Bentley *et al.*, 1986b; Phillips *et al.*, 1986; Purdy *et al.*, 1996; Plummer *et al.*, 1997; Davis *et al.*, 1998, 2000] have considered this source of error in detail. In addition, ^{36}Cl is produced naturally in the subsurface by the neutron activation of stable ^{35}Cl present in solution [Lehmann *et al.*, 1993]



The effect of this subsurface production on calculated age depends on groundwater chlorinity and the subsurface neutron flux. For very dilute groundwater, in which there is little subsurface production, the resulting error is commonly taken to be small [Purdy *et al.*, 1996].

[7] Less well understood is the extent to which transport phenomena in the subsurface can affect the calculation of ^{36}Cl ages (Figure 1). Chlorine 36 might be lost from an aquifer by diffusion into aquitards containing little of the isotope or gained from fine-grained sediments where the rate of subsurface production is high. Cross-formational flow can enrich or deplete the isotope. In addition, mixing of young and old groundwater can produce ^{36}Cl ages unlike the averaged age of the mixed waters, as described in the next section. In this paper, we use quantitative

modeling techniques to consider how transport phenomena might affect calculated ^{36}Cl ages.

2. The ^{36}Cl Dating Method

[8] The dating method works by tracking the radioactive decay of ^{36}Cl along a groundwater flow path. Cosmic rays produce ^{36}Cl in the atmosphere naturally by the spallation of Ar (Figure 1). The ^{36}Cl resides in the troposphere about a week on average before dissolving in rainfall [Faure, 1986], some of which recharges the subsurface. The atmospheric ^{36}Cl may be concentrated in groundwater within the soil zone, owing to the effects of evapotranspiration. Once water has infiltrated the subsurface beyond the soil zone, its initial ^{36}Cl content decreases because of radioactive decay, which occurs at a constant rate, regardless of physical and chemical conditions.

2.1. Radioactive Decay and Subsurface Production

[9] The concentration C of ^{36}Cl in a closed system, such as an isolated packet of groundwater migrating through a flow system (the "piston flow" model), decreases as a function of time according to the exponential decay function:

$$C = C_0 e^{-\lambda t}, \quad (2)$$

where C_0 is initial concentration and λ is the decay constant ($\lambda = \ln 2/T_{1/2}$; Figure 2a).

[10] Chlorine 36 not only decays but is produced naturally in the subsurface by the neutron activation of dissolved ^{35}Cl , the dominant stable isotope of the element, by neutrons released as a result of the radioactive decay of U and Th and their alpha-decay progeny. The isotope is also produced by activation of ^{35}Cl bound within minerals, but it appears unlikely that rock grains in an aquifer release enough of the isotope to affect our calculations

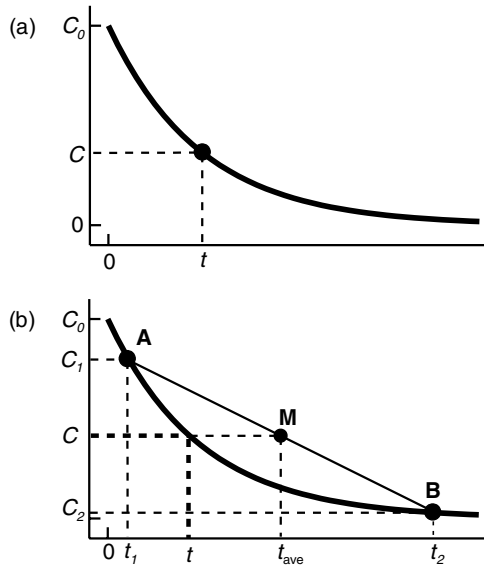


Figure 2. Calculation of groundwater age from ^{36}Cl concentration: (a) ^{36}Cl concentration decreases with time from its initial value C_0 . Age t can be calculated from concentration C , according to equation (5). (b) Fluid is a mixture “M” of two groundwaters “A” and “B” of ages t_1 and t_2 , which have ^{36}Cl concentrations C_1 and C_2 . Mixtures lie along straight line AB, because both age (t_{ave}) and concentration are simple averages. The ^{36}Cl age t calculated using equation (5) assumes the ^{36}Cl concentration C reflects aging of the water along the decay curve, not mixing along AB. The isotopic age t for a mixed fluid therefore is invariably less than the actual age t_{ave} .

[Purdy *et al.*, 1996]; hence we do not account for this possible source of ^{36}Cl to groundwater.

[11] The rate of subsurface production is proportional to the flux of neutrons, which depends on the composition of the rock grains, and to the concentration of dissolved ^{35}Cl . Neutrons are produced when light elements in the rock are bombarded with alpha particles, which are the products of the alpha decay chains of U and Th; neutrons are also produced by the spontaneous fission of ^{238}U . Within 50 m of the surface, as well, neutrons may be produced by primary cosmic rays and secondary pions and muons [Andrews *et al.*, 1991]. Groundwater in our models resides only briefly within this zone, however, so we do not account for this effect in our calculations.

[12] Since the alpha particles generated by the U and Th decay chains travel only a few microns through the subsurface, the nature of the U and Th distribution in the rock, such as whether the elements are distributed through the rock grains or localized in oxide coatings on grain surfaces, might be expected to affect the neutron flux and hence ^{36}Cl production. Lehmann *et al.* [1993], however, found reasonable agreement between inferred ^{36}Cl production rates and those calculated from rock composition, assuming homogeneous U and Th distributions. As such, and since there is no established basis for doing so, we do not account in our calculations for any possible effect of such heterogeneity.

[13] The rate P_{36} of ^{36}Cl production by the alpha decay chains of U and Th is proportional to the neutron flux multiplied by the ^{35}Cl neutron capture cross section. This rate, expressed in mol cm^{-3} of porous medium yr^{-1} , is

$$P_{36} = \Phi_n \phi \chi_{35} \sigma_{35} C_{\text{Cl}}, \quad (3)$$

where Φ_n is neutron flux, ϕ is porosity, χ_{35} is ^{35}Cl abundance (0.75775), σ_{35} is the neutron capture cross section of ^{35}Cl ($43.74 \times 10^{-24} \text{ cm}^2$), and C_{Cl} is Cl concentration (mol cm^{-3} water). The Appendix shows the method used to calculate the neutron flux from sediment composition; we use equation (3) to compute the ^{36}Cl production rate from the rate of neutron production.

[14] Because ^{36}Cl is produced as well as decays in the subsurface, it can achieve a state of secular equilibrium at which the rates of production and decay balance. In a closed system the isotope abundance R^{36} (the ratio of ^{36}Cl to chloride concentration) can be calculated by combining the isotope decay rate λC with equation (3) to give

$$R_{\text{se}}^{36} = \frac{\Phi_n \chi_{35} \sigma_{35}}{\lambda}, \quad (4)$$

Evaluating this expression using the data above and in Table 1 gives secular equilibrium ratios of 6.1×10^{-15} and 12×10^{-15} for a typical sandstone aquifer and a shale aquitard, respectively.

2.2. Calculation of Groundwater Age

[15] The residence time or age of a sample of groundwater can be calculated if the sample can be assumed to have behaved as an isolated packet when it migrated through the flow system (the piston flow model). In this case, ^{36}Cl concentration decreases as a function of time according to equation (2). Rearranging this equation, residence time t can be calculated from C and C_0

$$t = -\frac{1}{\lambda} \ln \frac{C}{C_0} \quad (5)$$

or, equivalently, from isotope abundances [Phillips *et al.*, 1986]

$$t = -\frac{1}{\lambda} \ln \frac{R^{36}}{R_0^{36}}, \quad (6)$$

where R^{36} is the ratio of $^{36}\text{Cl}/\text{Cl}$ and R_0^{36} is the initial value of this ratio.

[16] Subsurface production of ^{36}Cl can affect the interpretation of groundwater age, especially for older groundwater. Where the

Table 1. Boundary Conditions and Source Rates for ^{36}Cl and Chloride

Parameter	Value
Sediment U concentration ^a	
Aquitards	3.2 ppm
Aquifer	1.4 ppm
Sediment Th concentration ^a	
Aquitards	11.7 ppm
Aquifer	3.9 ppm
^{36}Cl production rate ^b	
Aquitards	$8 \times 10^{-26} \text{ mol cm}^{-3} \text{ yr}^{-1}$
Aquifer	$4 \times 10^{-26} \text{ mol cm}^{-3} \text{ yr}^{-1}$
Basin top surface	
^{36}Cl concentration	$2 \times 10^{-16} \text{ molal}$
Cl concentration	23 mg kg^{-1} ($6.5 \times 10^{-4} \text{ molal}$)
Basal boundary	
^{36}Cl flux	none
Cl concentration	1200 mg kg^{-1} ($3.4 \times 10^{-2} \text{ molal}$)

^aFaure [1986].

^bAs calculated from U and Th concentrations given, assuming groundwater Cl concentration = 100 mg kg^{-1} ; rate in simulations varies across domain with chlorinity. Expressed per cm^3 groundwater.

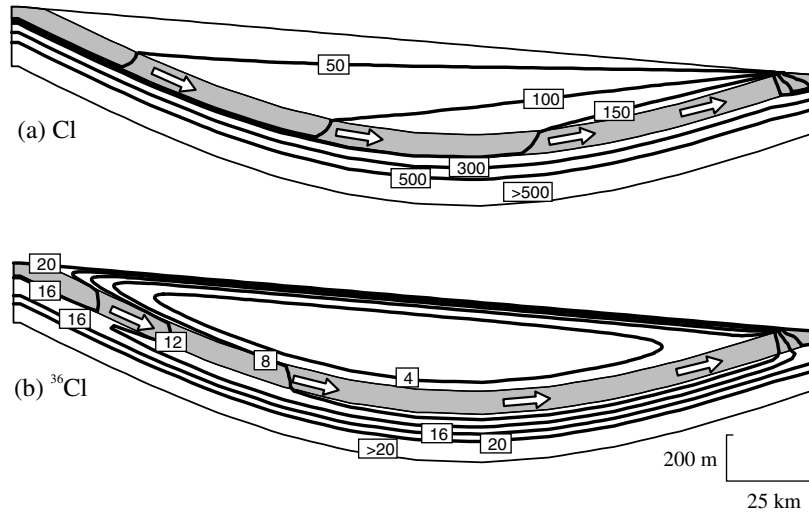


Figure 3. Model of groundwater flow along a cross section through a simple sedimentary basin. Topographic relief sets up groundwater flow through basin sediments, which consist of a sandstone aquifer confined above and below by shale aquitards: distribution of (a) chloride (isocons in mg kg^{-1}) and (b) ^{36}Cl (molal, $\times 10^{17}$).

production rate is uniform over the domain, equations (5) and (6) can be modified to account for the effect of subsurface production

$$t = -\frac{1}{\lambda} \ln \left(\frac{C^{36} - C_{se}^{36}}{C_0^{36} - C_{se}^{36}} \right) \quad (7)$$

$$t = -\frac{1}{\lambda} \ln \left(\frac{R^{36} - R_{se}^{36}}{R_0^{36} - R_{se}^{36}} \right). \quad (8)$$

Here, C_{se}^{36} and R_{se}^{36} are ^{36}Cl concentration and the $^{36}\text{Cl}/\text{Cl}$ ratio at secular equilibrium. As noted by *Torgersen et al.* [1991] and *Phillips et al.* [1986], such formulas are not valid when chlorinity varies along the flow line; therefore, we do not employ these relations in this study.

2.3. Effect of Subsurface Mixing

[17] Implicit in calculating age with these equations is the assumption that the groundwater packet has behaved as a closed system. If a sample is a mixture of two groundwaters of differing age, for example, the age t predicted by these equations differs from the weighted average age t_{ave} of the groundwaters. The discrepancy arises because the ^{36}Cl concentration decays along not a linear but a negative exponential trend, according to equation (2).

[18] Since groundwater in an impermeable layer might be orders of magnitude older than in a permeable layer nearby, it may be nearly devoid of atmospheric ^{36}Cl . Mixing a small amount of water from the aquitard into the aquifer increases the average groundwater age there significantly, but has a lesser effect on the ^{36}Cl age of the mixture, as illustrated in Figure 2b.

3. Model of ^{36}Cl Transport

[19] We model the transport of dissolved chloride and the ^{36}Cl isotope in a groundwater flow regime within an idealized large sedimentary basin. To perform the calculations, we use the Basin2 software package [*Bethke*, 1985; *Bethke et al.*, 1999a], available from <http://www.geology.uiuc.edu/Hydrogeology>. The modeling accounts for groundwater flow arising from topographic relief

and the resulting mass transport owing to diffusion, advection, and hydrodynamic dispersion.

3.1. Groundwater Flow and Piston Flow Age

[20] We model flow along a cross section, 240 km long and ~ 700 m deep, composed of a sandstone aquifer overlain and underlain by shale aquitards (Figure 3). 300 m of relief across the basin surface sets up a constant hydraulic gradient of 1:800 (0.125%) from left to right. The left and right sides are taken as no-flow boundaries, as is bottom of the basin, beneath the lower aquitard. Since we are interested in long-term behavior of the system, the model is calculated assuming steady state conditions.

[21] In our initial model the hydraulic conductivity of the aquifer is $10^{-4} \text{ cm s}^{-1}$ and porosity there is 15% (Table 2). The resulting groundwater velocity along the flow path is $\sim 26 \text{ cm yr}^{-1}$. The hydraulic conductivities of the upper and lower aquitards are 10^{-7} and $10^{-8} \text{ cm s}^{-1}$, respectively, and porosity in each is set to 20%.

[22] Groundwater age is the average time elapsed since water molecules at a position in the basin recharged the subsurface [*Fritzel*, 1996; *Goode*, 1996; *Varni and Carrera*, 1998; *Etcheverry and Perrochet*, 2000]. A simple conceptualization of groundwater age commonly held by hydrologists is the piston flow age, which is the time interval since recharge required for flow along a stream tube to reach a point in the subsurface. Where the longitudinal flow velocity v_x is constant over an aquifer, piston flow age is simply distance from

Table 2. Hydrologic Parameters Assumed in Calculations, Unless Noted

Parameter	Value
Hydraulic conductivity	
Upper aquitard	$10^{-7} \text{ cm s}^{-1}$
Aquifer	$10^{-4} \text{ cm s}^{-1}$
Lower aquitard	$10^{-8} \text{ cm s}^{-1}$
Porosity	
Aquifer	15%
Aquitards	20%
Dispersivity	
Longitudinal	1000 cm
Transverse	100 cm
Diffusion coefficient	
Chloride, ^{36}Cl	$10^{-6} \text{ cm}^2 \text{ s}^{-1}$

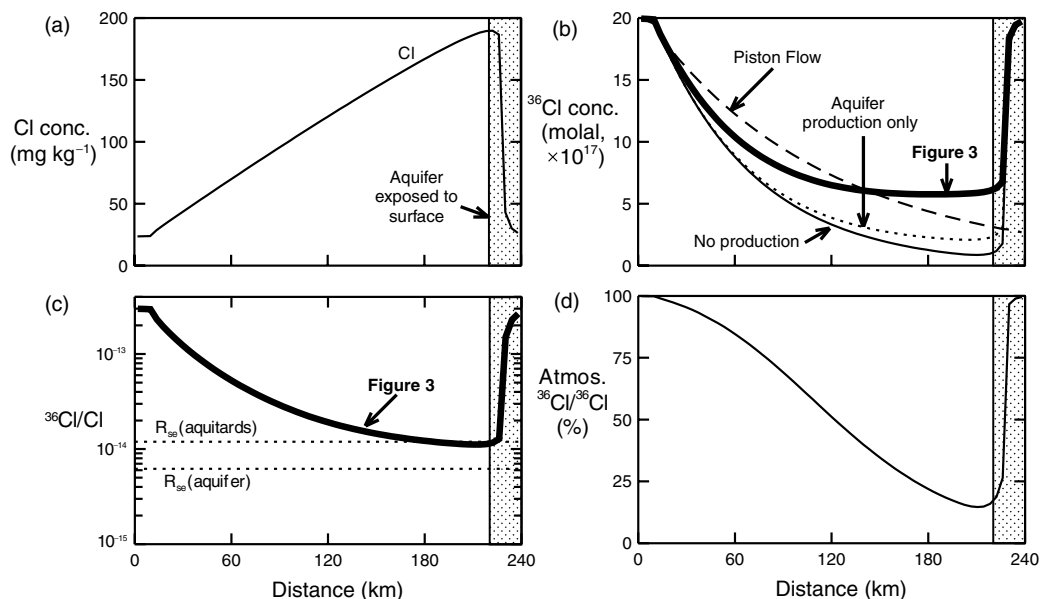


Figure 4. Concentrations of chloride and ^{36}Cl along the top of the aquifer (the concentrations vary little with vertical position in the aquifer, owing to the effects of lateral dispersion) for the simulation shown in Figure 3. The stippled area at the right of the plots shows where the aquifer in the discharge area is exposed to the atmosphere. The ^{36}Cl and Cl concentrations and calculated isotope ages here reflect the upper boundary conditions; for clarity, we omit this region from subsequent figures. (a) Variation in chloride concentration. (b) Predicted ^{36}Cl concentration (bold line) for simulation, compared to that calculated ignoring subsurface production of the isotope (thin line), and production within the aquifers alone (dotted line); dashed line shows the profile expected from simple radioactive decay (the “piston flow” model). (c) Chlorine 36 abundance (the $^{36}\text{Cl}/\text{Cl}$ ratio), compared to secular equilibrium ratio in the aquifer and aquitards, the latter being richer in U and Th. (d) Fraction of ^{36}Cl reservoir of atmospheric origin, determined as the ratio of ^{36}Cl in a model neglecting subsurface production to one accounting for it.

the recharge area divided by velocity. More generally, piston flow age $\tau(l)$ at a position l along the flow path is given by

$$\tau(l) = \int_0^l \frac{dx}{v_x} \quad (9)$$

This quantity is significant in groundwater studies because its derivative gives flow velocity along the flow path directly. In our simulations, piston flow age in the aquifer ranges from zero at recharge to $\sim 900,000$ year, approximately the upper limit of ages suitable for ^{36}Cl dating, near the discharge area.

3.2. Distribution of Chloride and ^{36}Cl

[23] We set boundary conditions for chloride transport on the basis of the observed distribution of chlorinity in the “J” aquifer of the Great Artesian Basin of Australia [Bentley *et al.*, 1986b]. Along the upper boundary, we specify a Cl concentration of 23 mg kg^{-1} (6.5×10^{-4} molal). This value represents the chloride content of recharging groundwater, after concentration by evapotranspiration in the soil zone. There is in the calculations no chloride flux across the side boundaries.

[24] Chlorinity in sedimentary basins generally increases with depth, commonly along a diffusive gradient [Sathaye and Grandstaff, 1996]. As a result, chlorinity in regional flow regimes tends to increase along flow paths as Cl diffuses from depth and mixes into migrating groundwater [Domenico and Schwartz, 1990]. To simulate this effect, we set a chloride concentration of 1200 mg kg^{-1} (3.4×10^{-2} molal) along the base of the cross section. Chloride in the model diffuses upward across the lower aquitard into the aquifer, causing chlorinity there to increase along the direction of flow. Chlorinity in the calculation, as in the Great Artesian Basin, reaches a value of 190 mg kg^{-1} (5.4×10^{-3} molal) near the discharge area.

[25] For ^{36}Cl we set an upper boundary condition of 2×10^{-16} molal, which is about the concentration in recharging groundwater in the Great Artesian Basin [Torgersen *et al.*, 1991] and the Milk River aquifer of the Western Canada Sedimentary Basin [Nolte *et al.*, 1991]. There is no flux of ^{36}Cl across the model’s side or lower boundaries (since the isotope can diffuse only a short distance through the basal aquitard during its half-life, as discussed later, the basal ^{36}Cl flux does not affect concentration in the aquifer). ^{36}Cl is assumed to be produced in situ within basin sediments by neutron activation at the rate given by equation (3), assuming sediment U and Th concentrations shown in Table 1 [Faure, 1986]. A_1 and A_2 values (equation (16)) for the aquifer are set to 0.996 and 0.2458 neutrons $\mu\text{g}^{-1} \text{ yr}^{-1}$, and for the aquitards to 1.34 and 0.4091 neutrons $\mu\text{g}^{-1} \text{ yr}^{-1}$.

[26] We take transverse and longitudinal dispersivities α_T and α_L , respectively, of 10^2 and 10^3 cm. We further assume a porous medium coefficient of molecular diffusion D^* of $10^{-6} \text{ cm}^2 \text{ s}^{-1}$ for both ^{36}Cl and chloride, as suggested by values for chloride measured in shale near room temperature [Barone *et al.*, 1990; Hendry *et al.*, 2000]. The coefficient of hydrodynamic dispersion is a tensor quantity with entries D_{xx} , D_{xz} , D_{zx} , and D_{zz} ($\text{cm}^2 \text{ s}^{-1}$) given by

$$D_{xx} = D^* + \alpha_T v + (\alpha_L - \alpha_T) \frac{v_x^2}{v}, \quad (10)$$

$$D_{xz} = D_{zx} = (\alpha_L - \alpha_T) \frac{v_x v_z}{v}, \quad (11)$$

$$D_{zz} = D^* + \alpha_T v + (\alpha_L - \alpha_T) \frac{v_z^2}{v}. \quad (12)$$

Here v is the magnitude of groundwater velocity (cm s^{-1}) and v_x and v_z are its components along and across stratigraphy. The components

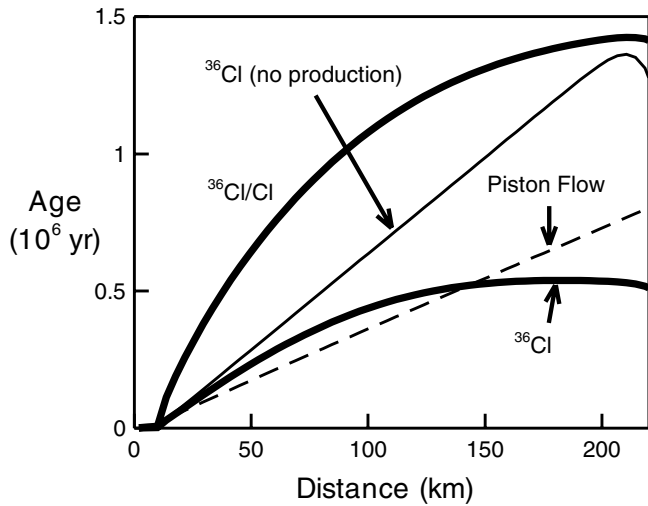


Figure 5. Chlorine 36, and $^{36}\text{Cl}/\text{Cl}$ ages (bold lines) calculated according to equations (5) and (6), compared to piston flow age (dashed line). Thin line shows ^{36}Cl age derived from a model calculated neglecting subsurface production of the isotope.

of the diffusive-dispersive flux ($\text{mol cm}^{-2} \text{s}^{-1}$) are then given

$$q_{D_x} = -\phi \left(D_{xx} \frac{\partial C}{\partial x} + D_{xz} \frac{\partial C}{\partial z} \right) \quad (13)$$

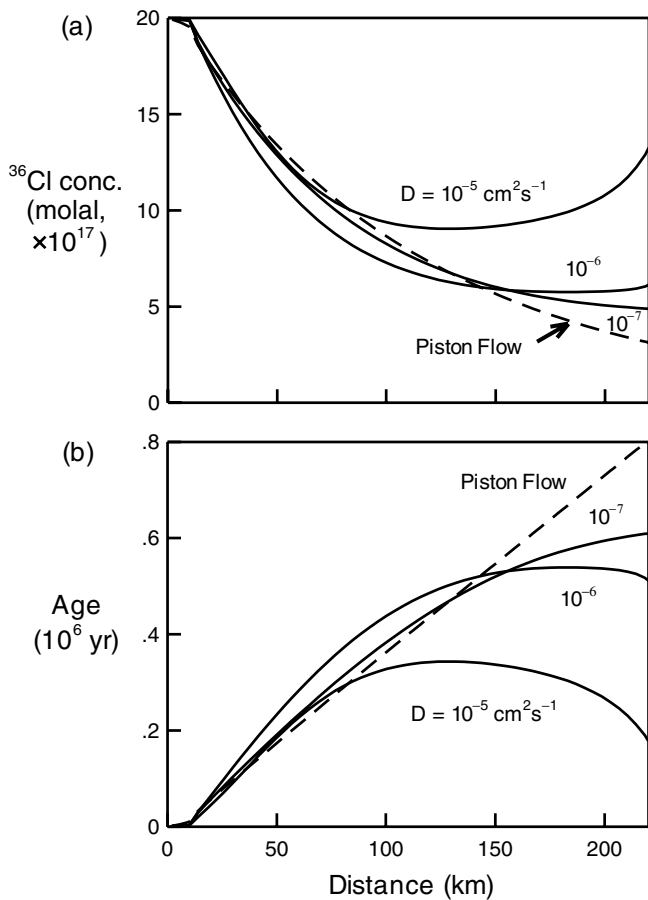


Figure 6. Effect along the aquifer of choice of diffusion coefficient on (a) ^{36}Cl concentration and (b) groundwater age calculated according to equation (5).

$$q_{D_z} = -\phi \left(D_{zx} \frac{\partial C}{\partial x} + D_{zz} \frac{\partial C}{\partial z} \right). \quad (14)$$

4. Results and Discussion

[27] Figure 3 shows how the concentrations of chloride and ^{36}Cl in the calculation results vary across the basin. Chloride in the model diffuses upward across the lower aquitard, where it is most concentrated, into the aquifer. As a result, groundwater flowing through the aquifer increases in chlorinity from 23 mg kg^{-1} at recharge to $\sim 190 \text{ mg kg}^{-1}$ near the discharge area (Figure 4a).

[28] Groundwater in the model results is rich in atmospheric ^{36}Cl along the basin surface and in the aquifer near the recharge area. A second area of high ^{36}Cl concentration occurs at depth in the lower aquitard, where groundwater is more saline than elsewhere in the basin. The relatively high rate of subsurface production here and the slow rate at which solutes can diffuse through the shale allow the isotope to accumulate. In contrast, ^{36}Cl is least concentrated within the upper aquitard, where groundwater is old and salinity (and hence the rate of subsurface production) is low.

[29] As groundwater flows through the aquifer away from the recharge area, the ^{36}Cl concentration diminishes owing to radioactive decay (Figure 4b). Atmospheric ^{36}Cl is also lost from the aquifer by diffusion into the aquitards, and, to a lesser extent, diluted by cross-formational flow. Deep in the basin, diffusion

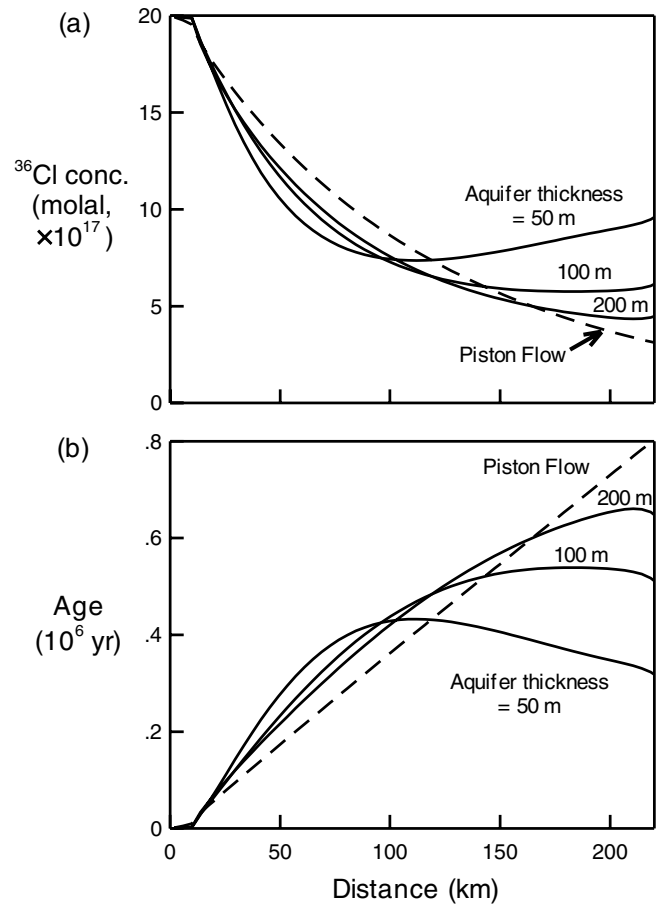


Figure 7. Effect along the aquifer of aquifer thickness on (a) ^{36}Cl concentration and (b) groundwater age calculated according to equation (5).

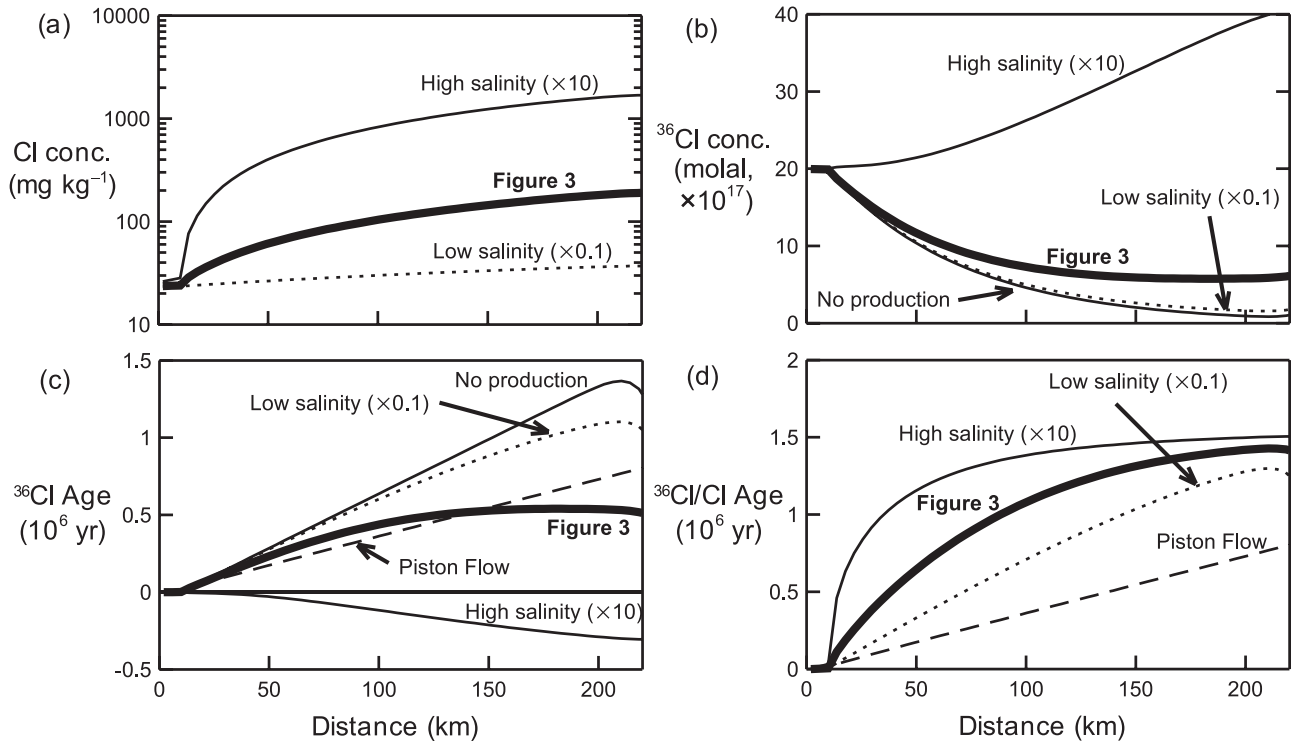


Figure 8. Variation in (a) chloride concentration, (b) ^{36}Cl concentration, (c) calculated ^{36}Cl age, and (d) calculated $^{36}\text{Cl}/\text{Cl}$ age along the aquifer for simulations similar to that shown in Figure 3 but with varying salinity in the underlying aquitard.

from the underlying aquitard, which contains more U, Th, and Cl than the aquifer, and where groundwater is more saline, contributes ^{36}Cl to the aquifer. Only a relatively thin portion of the aquitard supplies ^{36}Cl to the aquifer because the isotope can diffuse just a limited distance before it decays. We can estimate the thickness of this layer as the diffusion length $\ell = \sqrt{D^*t}$, where D^* is the diffusion coefficient and t is the isotope's half-life (301,000 years). Taking D^* to be $10^{-6} \text{ cm}^2 \text{ s}^{-1}$, we can expect ^{36}Cl to be derived from the 30 m thickness of aquitard adjacent to the aquifer.

[30] Near the center of the basin, the rate of radioactive decay becomes balanced by the rate at which the isotope is supplied by diffusion into the aquifer. Here, ^{36}Cl concentration becomes almost invariant at a value in excess of that expected at secular equilibrium (Figure 4c). The $^{36}\text{Cl}/\text{Cl}$ ratio within the aquifer never reaches secular equilibrium for two reasons. First, insufficient time elapses as groundwater traverses the aquifer, given the isotope's half-life. Second, ^{36}Cl and Cl diffuse continuously from the underlying aquitard, which is richer in U, Th, and Cl than the aquifer. Groundwater here has reached secular equilibrium and hence has a $^{36}\text{Cl}/\text{Cl}$ ratio higher than would be found at equilibrium in the aquifer.

[31] As a result of this pattern of decay and accumulation, the fraction of ^{36}Cl derived from the atmosphere decreases sharply as groundwater flows along the aquifer (Figure 4d). This is notable because the basis of ^{36}Cl age dating, atmospheric ^{36}Cl , makes up a diminishing fraction of the ^{36}Cl content of groundwater along the flow path.

[32] The lower aquitard in the deep basin contributes more ^{36}Cl to the aquifer than is produced within the aquifer itself. This effect is shown clearly in Figure 4b, where ^{36}Cl concentration calculated neglecting production within the aquitards is considerably less than in the full model, but close to that of a model

neglecting subsurface production entirely. Previous studies [e.g., Bentley *et al.*, 1986b; Phillips *et al.*, 1986; Nolte *et al.*, 1991; Torgersen *et al.*, 1991] have considered how ^{36}Cl production within the aquifer affects dating studies. Our modeling suggests that we need to account for production of the isotope within surrounding aquitards as well.

[33] These calculations suggest a simple but approximate method for estimating the salinity limit to ^{36}Cl dating. If most of the chloride in an aquifer has diffused from surrounding aquitards, the aquitards have contributed ^{36}Cl to the aquifer in a concentration of about $R_{se} \cdot C_{\text{Cl}}$, where R_{se} is the secular equilibrium ratio in the aquitard and C_{Cl} is aquifer chlorinity. Setting this concentration equal to that of the atmospheric ^{36}Cl at recharge, C_{36}^0 , remaining after n half lives of transit gives

$$C_{\text{Cl}} = \frac{C_{36}^0 (1/2)^n}{R_{se}}, \quad (15)$$

which is the approximate salinity at which ^{36}Cl produced in the subsurface overwhelms the atmospheric contribution. If we wish to apply ^{36}Cl dating over 2–3 half lives of the isotope, for example, then taking C_{36}^0 to be 2×10^{-16} molal and an R_{se} of 12×10^{-15} , as in our models, suggests that the dating cannot be applied reliably for the conditions considered where groundwater chlorinity exceeds ~ 75 – 150 mg kg^{-1} .

4.1. Isotopic Versus Piston Flow Age

[34] Figure 5 shows how groundwater ages from the predicted ^{36}Cl concentration and abundance ($^{36}\text{Cl}/\text{Cl}$ ratio) using equations (5) and (6) compare along the aquifer to the piston flow

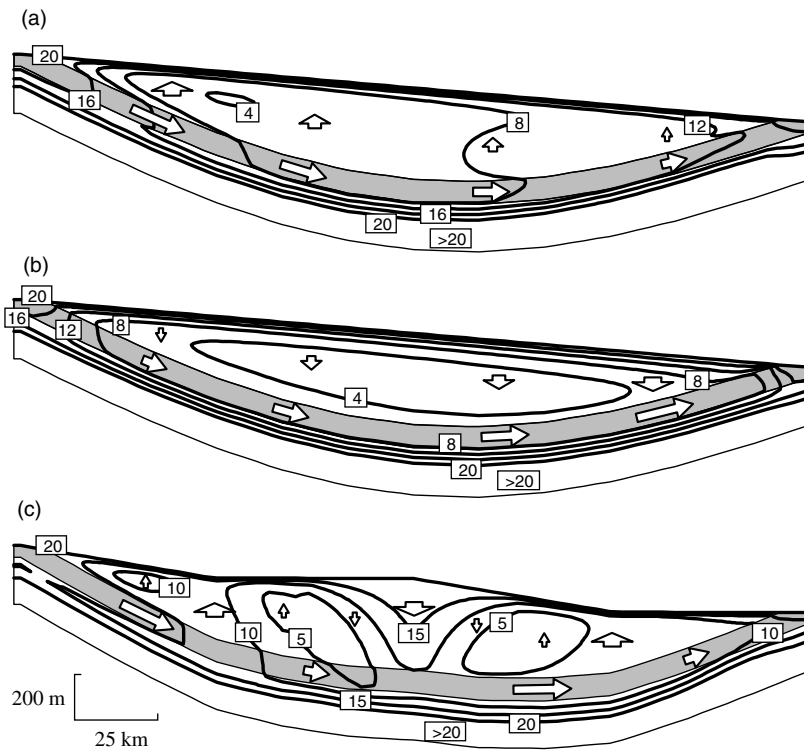


Figure 9. Simulations of ^{36}Cl transport (^{36}Cl isocons in molal, $\times 10^{17}$) for basins with significant cross-formational flow across the upper aquitard: (a) hydraulic conductivity decreases along the aquifer, creating a broad area of discharge across the aquitard; (b) conductivity follows the opposite pattern (increases along flow), creating a broad recharge area; and (c) an irregular slope on the water table produces subregional flow cells superimposed on the regional regime.

age of groundwater in the transport model. Chlorine 36 concentration is affected by two competing processes: ^{36}Cl loss near the recharge area due to its diffusion into surrounding aquitards, and the gain deeper in the basin of ^{36}Cl produced in the aquifer and aquitards. The first process makes the ^{36}Cl age in recently recharged groundwater slightly older than the piston flow age (Figure 5). The second process maintains a plateau in ^{36}Cl concentration, and hence calculated age, deep in the basin. Depending on the amount of ^{36}Cl diffusing into an aquifer, therefore ^{36}Cl age determinations may become inaccurate after only about two half-lives have elapsed since recharge.

[35] The trend in ^{36}Cl age agrees rather well with piston flow age. This agreement results from the fact that over the scale of the basin the net addition of the isotope into the aquifer from below balances approximately with its loss upward. For the simple flow system considered, the net result of the ^{36}Cl transport model mirrors the piston flow concept, giving isotopic ages that resemble the piston flow age. We will see that this result is not necessarily maintained in more complex, and hence realistic, model configurations.

[36] Age calculated from the $^{36}\text{Cl}/\text{Cl}$ ratio at any point in the basin is older than that computed from the ^{36}Cl concentration (Figure 5) because of the diffusion of chloride from below. The $^{36}\text{Cl}/\text{Cl}$ ratio of this chloride is much lower than that of atmospheric recharge. Hence the mixing of this “dead” chloride into the aquifer reduces the ^{36}Cl abundance (the $^{36}\text{Cl}/\text{Cl}$ ratio) there, leading to older calculated ages.

[37] Where salinity is low, subsurface production is small and hence cannot counterbalance the diffusive loss of atmospheric

^{36}Cl into the aquitards, allowing the isotope within the aquifer to become depleted. The calculated ^{36}Cl age in this limiting case of no production (Figure 5) is $\sim 75\%$ larger than the piston flow age.

4.2. Role of Diffusion, Aquifer Thickness, and Aquitard Salinity

[38] We have assumed to this point a porous medium diffusion coefficient D^* , the product of the diffusion coefficient in water and sediment tortuosity, for chloride of $10^{-6} \text{ cm}^2 \text{ s}^{-1}$. Sediments, however, vary in tortuosity, and a range of values may apply in nature. In studies of the Milk River aquifer, for example, *Hendry and Schwartz* [1988] and *Nolte et al.* [1991] estimated a value of D^* for chloride in shale of $\sim 6 \times 10^{-8} \text{ cm}^2 \text{ s}^{-1}$.

[39] Figure 6 shows how the choice of diffusion coefficient affects ^{36}Cl concentration in the transport model. In each case we take the Cl distribution from the previous model (Figure 3), so that subsurface production rates do not vary among the model runs. Taking a larger coefficient of $10^{-5} \text{ cm}^2 \text{ s}^{-1}$ allows more ^{36}Cl to diffuse from depth and accumulate within the aquifer. The concentration of ^{36}Cl in the model results therefore is higher in ^{36}Cl and therefore of a younger isotope age than in the previous case. A smaller coefficient of $10^{-7} \text{ cm}^2 \text{ s}^{-1}$ restricts the supply of ^{36}Cl from diffusion. Chlorine 36 concentration in this case approaches the trend expected from the piston flow model and ^{36}Cl age approaches the piston flow age.

[40] The effect of diffusion on the ^{36}Cl distribution within an aquifer depends inversely on aquifer thickness: a given diffusive flux affects concentration more in a thin aquifer than in a thick

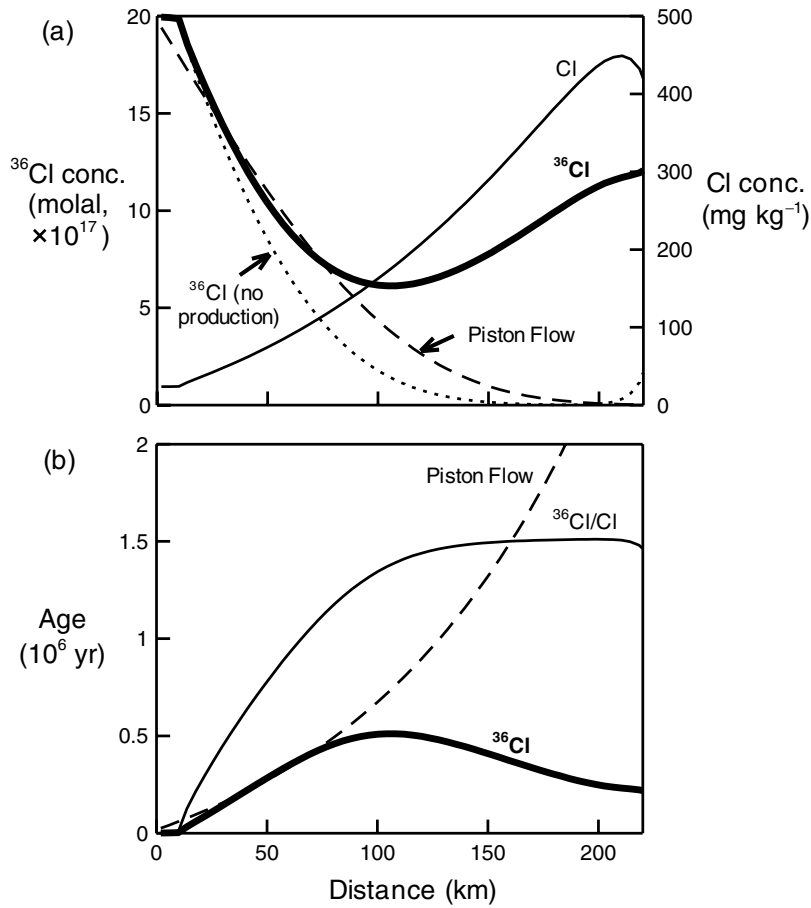


Figure 10. Model results for simulation shown in Figure 9a: (a) variation in ^{36}Cl (bold lines; molal, $\times 10^{17}$) and Cl concentrations (thin lines; mg kg^{-1}), and ^{36}Cl concentration expected from the piston flow model (dashed lines; molal, $\times 10^{17}$) along the aquifer; and (b) ages calculated using equations (5) and (6).

one. Figure 7 shows the results of simulations for aquifers of differing thickness, calculated assuming a diffusion coefficient D^* of $10^{-6} \text{ cm}^2 \text{ s}^{-1}$. Chlorine 36 concentration in these results approaches the piston flow model as aquifer thickness increases, much as it did in simulations (Figure 6) made assuming small diffusion coefficients. The extent to which diffusion affects ^{36}Cl age therefore depends on both the diffusion coefficient in neighboring aquitards and the thickness of the aquifer in question.

[41] Figure 8 shows how salinity in the underlying aquitard affects chloride content and isotopic composition in the aquifer. In a simulation in which salinity at the basal boundary is set a factor of 10 lower than in the reference simulation, the ^{36}Cl content and model ages approach the case already considered (Figure 4) in which there is no subsurface production. In a high-salinity simulation we set the basal chlorinity to a value ten times higher than in the reference model; the basal chlorinity in this case is approximately that of seawater. The results of this simulation differ broadly from those of previous simulations because the contribution to the aquifer of ^{36}Cl produced in situ within the aquitard comes to overwhelm the isotope's atmospheric contribution. The ^{36}Cl content of groundwater in the aquifer increases along the direction of flow, resulting in negative calculated ^{36}Cl ages. Reflecting the strong influence of chloride diffusion from the aquitard, $^{36}\text{Cl}/\text{Cl}$ age varies little across much of the aquifer,

simply reflecting the isotopic abundance within the aquitard at secular equilibrium.

4.3. Cross-formational Flow

[42] Figure 9 shows the ^{36}Cl distributions predicted for three scenarios in which cross-formational flow is more important than in the previous case (Figure 3). In the first scenario (Figure 9a) we consider a leaky aquifer in which hydraulic conductivity decreases from $10^{-4} \text{ cm s}^{-1}$ at recharge to $10^{-5} \text{ cm s}^{-1}$ in the discharge area. Confronted with decreasing conductivity, groundwater in the aquifer discharges upward across the confining layer, and velocity within the aquifer decreases with distance.

[43] Upgradient in the aquifer, ^{36}Cl concentration and age (Figures 10a and 10b) follow trends similar to those expected from the piston flow model. Downgradient, however, ^{36}Cl concentration deviates from the piston flow model, increasing along the direction of flow. Groundwater here moves more slowly than in the previous case (Figure 3) and hence accumulates chloride diffusing from below, which leads to a higher rate of subsurface production in the aquifer and neighboring aquitards, and hence greater ^{36}Cl concentrations. The ^{36}Cl age, as a result, fails to reflect the slow rates of flow.

[44] The $^{36}\text{Cl}/\text{Cl}$ age changes little in this part of the aquifer because the isotope abundance is controlled in large part by ^{36}Cl

and Cl diffusing from the aquitard below, where the abundance is close to secular equilibrium. Significantly smaller ^{36}Cl concentrations are predicted in a model calculated ignoring subsurface production (Figure 10a), reflecting the dominance in downgradient portions of the aquifer of ^{36}Cl derived in situ.

[45] The second case (Figure 9b) is the reverse of the first: an increase in conductivity from 10^{-5} to 10^{-4} cm s^{-1} across the aquifer produces a broad area of recharge. Groundwater in the aquifer moves slowly near the recharge area, and ^{36}Cl concentration there decreases sharply owing to radioactive decay (Figure 11a). Farther along the aquifer, the ^{36}Cl concentration varies little because ^{36}Cl diffusing from lower aquitard is diluted by groundwater recharging across the upper aquitard, which has become nearly depleted in the isotope during the time required to traverse the confining layer.

[46] As can be seen by comparing the model with a calculation made ignoring subsurface production (Figure 11a), ^{36}Cl produced in the subsurface dominates the ^{36}Cl reservoir in the aquifer. The

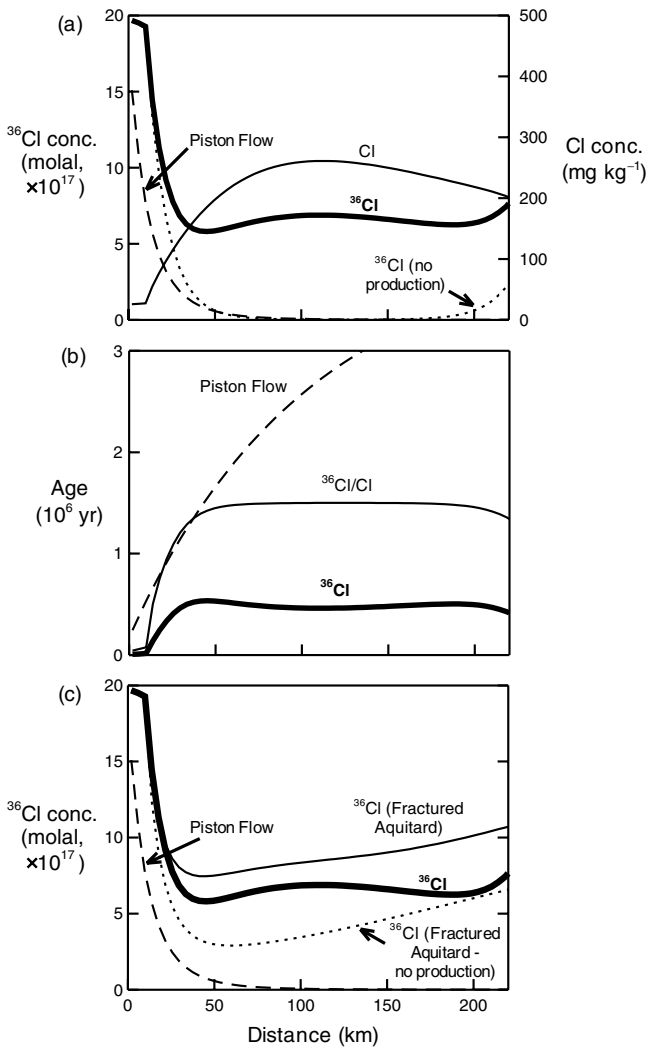


Figure 11. Model results for simulation shown in Figure 9b: (a) variation in ^{36}Cl (bold lines; molal, $\times 10^{17}$) and Cl concentrations (thin lines; mg kg^{-1}), and ^{36}Cl concentration expected from the piston flow model (dashed lines; molal, $\times 10^{17}$); (b) ages calculated using equations (5) and (6); and (c) results for a simulation in which flow through the aquitard occurs through fractures rather than the rock matrix.

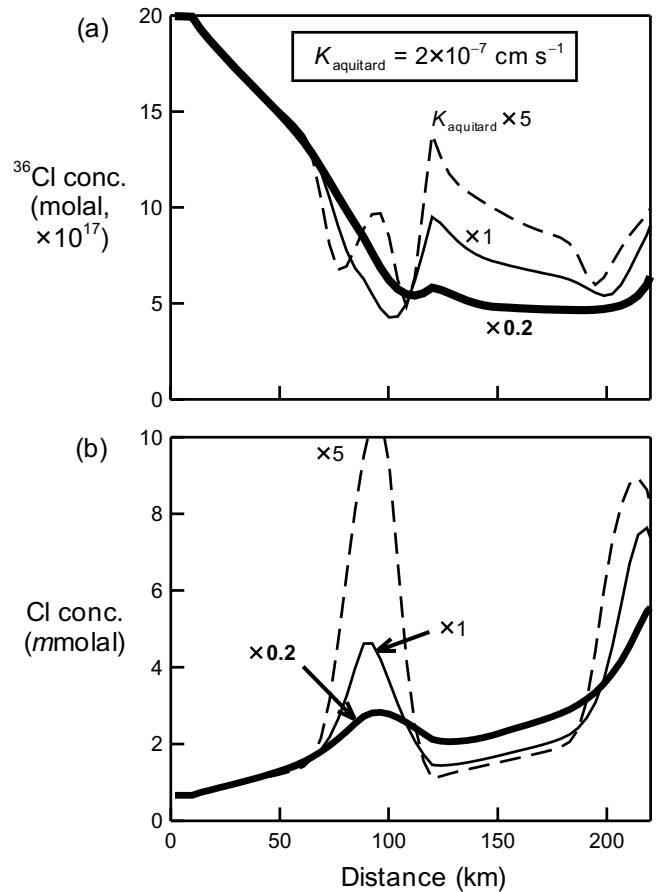


Figure 12. Model results for simulation shown in Figure 9c: (a) ^{36}Cl and (b) Cl concentrations along the aquifer for models calculated assuming various aquitard conductivities. The base model ($\times 1$, thin line) is calculated taking $K_{\text{aquitard}} = 2 \times 10^{-7} \text{ cm s}^{-1}$. Models for lower ($\times 0.2$, bold line) and higher ($\times 5$, dashed line) aquitard conductivities are calculated taking $K_{\text{aquitard}} = 4 \times 10^{-8} \text{ cm s}^{-1}$ and $10^{-6} \text{ cm s}^{-1}$.

^{36}Cl and $^{36}\text{Cl}/\text{Cl}$ ages (Figure 11b) are considerably younger than the piston flow age because of this subsurface production. The ages vary little across the aquifer and hence do not represent the velocity or even direction of flow there.

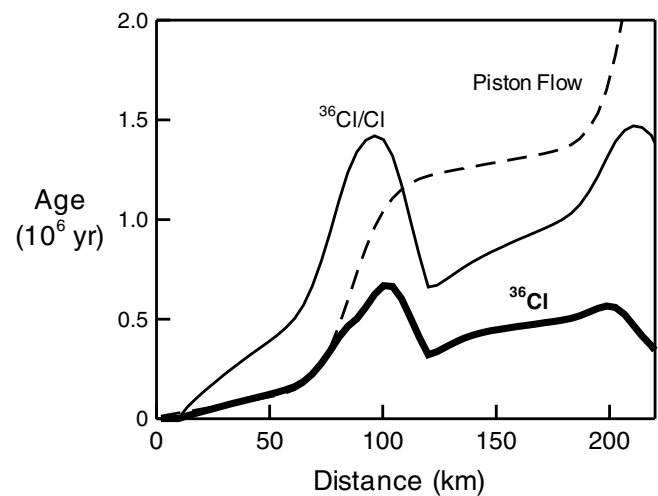


Figure 13. Chlorine 36 and $^{36}\text{Cl}/\text{Cl}$ ages for simulation shown in Figure 9c, as calculated using equations (5) and (6).

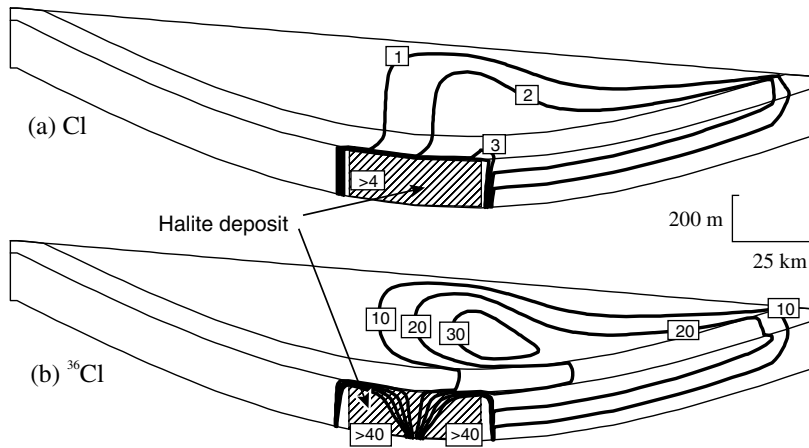


Figure 14. Distribution of (a) chlorinity (molal) and (b) ^{36}Cl (molal, $\times 10^{17}$) in a basin in which halite in an evaporite bed (patterned area) dissolves within the lower aquitard and diffuses into the aquifer, producing a solute plume. The pattern of ^{36}Cl concentration within the evaporite bed results from the downward and outward flow of dense, saline groundwater there.

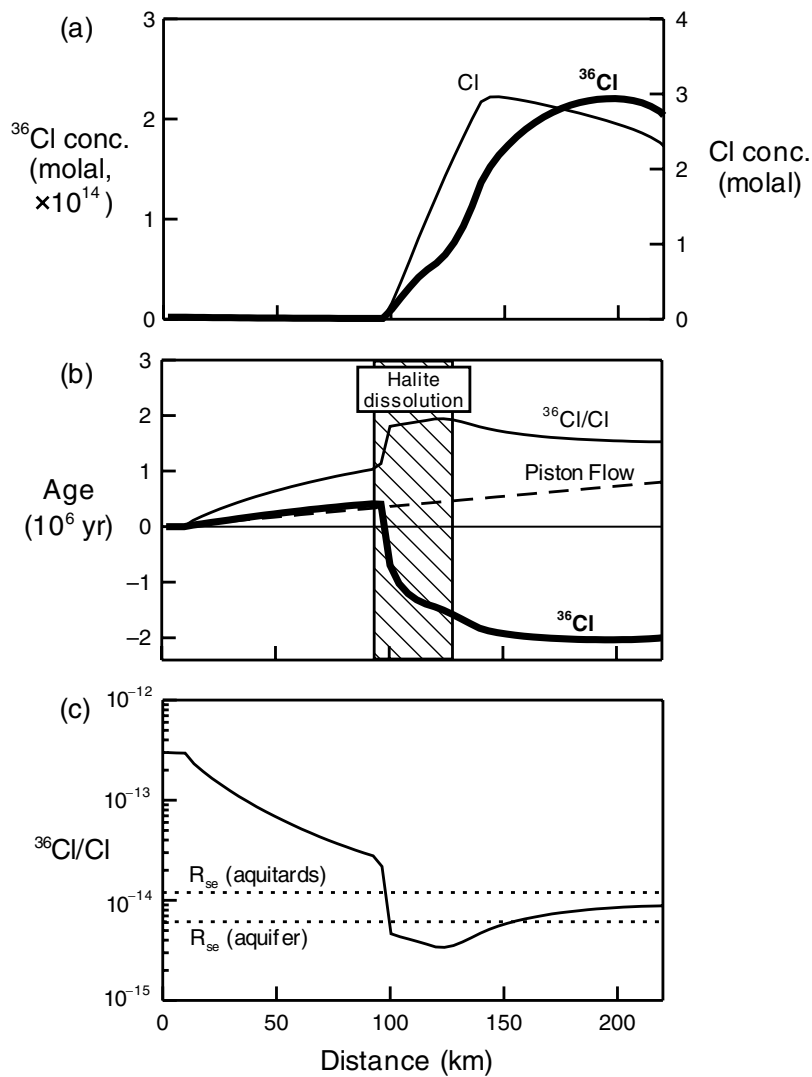


Figure 15. Variation in (a) ^{36}Cl and Cl concentration, (b) groundwater age, and (c) $^{36}\text{Cl}/\text{Cl}$ ratio along the aquifer, in the simulation shown in Figure 14.

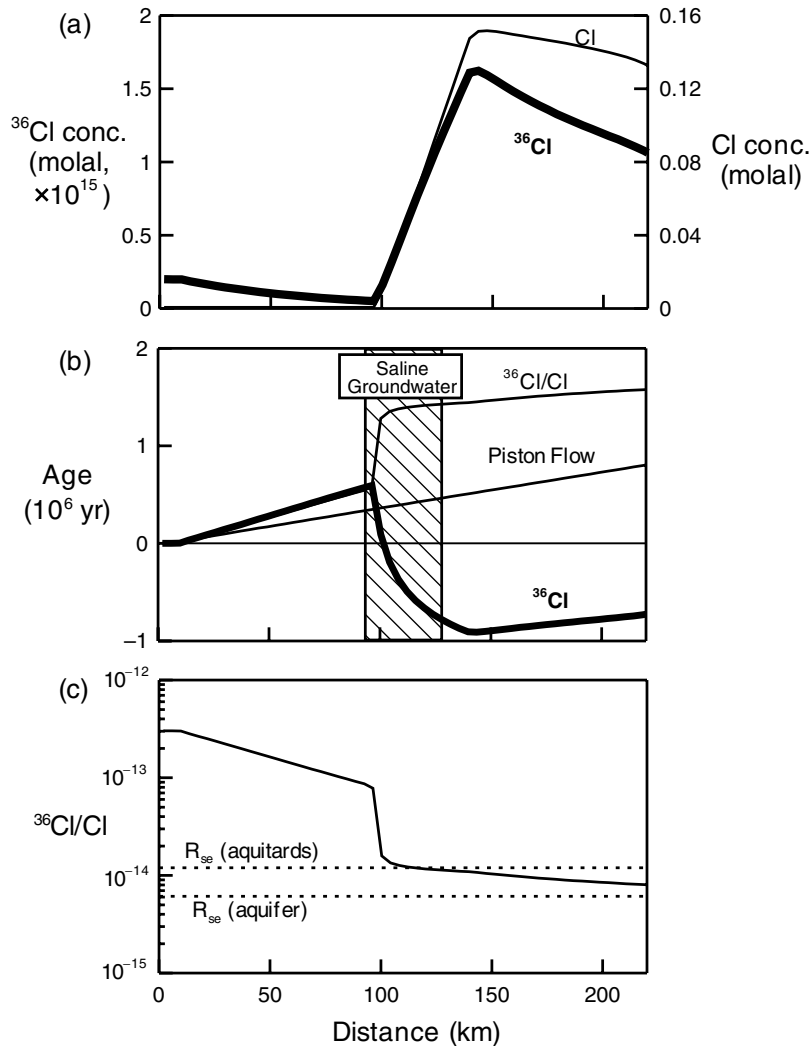


Figure 16. Variation in (a) ^{36}Cl and Cl concentration, (b) groundwater age, and (c) $^{36}\text{Cl}/\text{Cl}$ ratio along the aquifer in a simulation similar to that shown in Figure 14, except that the source of salinity is saline groundwater trapped in the underlying aquitard.

[47] In a variant on this scenario we consider the effects of fluid being transmitted across the upper aquitard through fractures, instead of through the sediment matrix. To calculate this model, we set porosity to a small value (0.1%) while maintaining conductivity as before. In the calculation results (Figure 11c), surface water traverses the confining layer rapidly enough to avoid significant decay of atmospheric ^{36}Cl . As a result, ^{36}Cl concentration in the aquifer is higher than the previous case (Figure 11a). Atmospheric ^{36}Cl dominates the reservoir of this isotope in the aquifer in this case, as can be seen by comparing it to a calculation made ignoring subsurface production (Figure 11c). Nonetheless, the distribution of ^{36}Cl does not reflect flow rate or direction within the aquifer.

[48] The third scenario (Figure 9c) accounts for the effects of an uneven slope on the water table. This configuration produces subregional flow cells that recharge and discharge across the upper aquitard at rates that depend on the value assumed for aquitard conductivity. For the reasons illustrated in the previous two scenarios, the cross-formational flow creates complex distributions of ^{36}Cl and Cl in the aquifer (Figure 12).

[49] Ages calculated from ^{36}Cl concentration or the $^{36}\text{Cl}/\text{Cl}$ ratio (Figure 13) differ significantly from the piston flow age. The

isotopic ages reach local maxima upgradient of the central recharge area and local minima beneath it, suggesting reversals of flow direction within the aquifer, where, in fact, no reversals exist. These effects are most pronounced in the simulation made assuming a relatively large value for aquitard conductivity.

4.4. Effect of Evaporite Beds and Trapped Saline Groundwater

[50] The presence of evaporite beds containing halite (and perhaps other chloride minerals) in the subsurface can drastically alter groundwater salinity and hence the distribution of ^{36}Cl in a flow regime. Since natural halite contains negligible U or Th, dissolving it can be expected to provide abundant stable Cl (^{35}Cl and ^{37}Cl) but little ^{36}Cl . As the dissolved salt migrates through the flow regime, however, neutron activation of ^{35}Cl in solution over time can produce significant amounts of ^{36}Cl .

[51] Figure 14 shows how chloride and ^{36}Cl vary across the basin for a scenario in which a body of halite in the lower aquitard dissolves into the groundwater flow. Halite is soluble at low temperature to a concentration of ~ 6 molal. In the model the halite dissolves and diffuses upward into the aquifer, creating a

plume in which chlorinity reaches ~ 3 molal and then gradually decreases along the direction of flow, owing to mixing.

[52] Chlorine 36 is produced relatively rapidly within the saline plume (Figure 15a), reaching concentrations several orders of magnitude greater than in atmospheric recharge. As a result, using equation (5) to calculate age for this groundwater gives negative values (Figure 15b). Ages calculated from the $^{36}\text{Cl}/\text{Cl}$ ratio (equation (6)) become significantly older as groundwater approaches the zone of halite dissolution and incorrectly decrease along the direction of flow within the plume.

[53] The $^{36}\text{Cl}/\text{Cl}$ ratio within the plume is small and increases downgradient (Figure 15c), suggesting that groundwater influenced by evaporite beds within about the past 10^5 years may be identified by the combination of high chlorinity and low $^{36}\text{Cl}/\text{Cl}$. *Andrews et al.* [1986, 1989], for example, identified such lower than expected $^{36}\text{Cl}/\text{Cl}$ ratios in the Stripa granite. These results serve to emphasize the added complexity entailed in applying ^{36}Cl dating method to basins containing saline groundwater.

[54] Figure 16 shows the results of a model in which the source of salinity is a pool of saline water trapped at depth. This case differs from the halite case (Figure 14) in that the chloride is contained in the pore space of the aquitard and thus contains considerable ^{36}Cl as the result of subsurface production. The predicted ^{36}Cl and $^{36}\text{Cl}/\text{Cl}$ ages in this case differ less markedly from the piston flow age than in the halite case, and do not decrease along the direction of flow. The ^{36}Cl method, nonetheless, produces negative ages, and neither method predicts ages that reflect flow conditions in the aquifer.

5. Conclusions

[55] The transport simulations presented in this paper demonstrate that mass transport phenomena and subsurface production can significantly affect the distribution of ^{36}Cl in regional groundwater flow regimes, and thereby influence the interpretation of ^{36}Cl groundwater age. The modeling demonstrates the following:

1. Under optimum conditions, age calculated from ^{36}Cl concentration can closely reflect a groundwater's piston flow age. Factors favoring this correspondence include low salinity, insignificant cross-formational flow, a thick aquifer, and a small diffusion coefficient in neighboring aquitards.

Table 3. Tables of Values Assumed in Calculation

Element	Mass Stopping Power ^a	Mass Fraction ^b		Neutron Yields ^c	
		Sandstone	Shale	U	Th
H	1779	0.0018	0.0060	0	0
C	635	0.48	0.16
O	609	0.5342	0.5341	0.24	0.08
F	531	0.0003	0.0008	31.60	12.50
Na	503	0.0034	0.0103	12.50	5.75
Mg	520	0.0072	0.0162	5.52	2.33
Al	493	0.0256	0.0861	4.88	2.39
Si	501	0.3766	0.2940	0.68	0.32
K	455	0.0109	0.0286	0.37	0.09
Ca	453	0.0400	0.0238	<.01	<.01

^a*Feige et al.* [1968].

^b*Parker* [1967].

^c*Andrews et al.* [1989]. Units of neutrons per a μg of U and Th per yr. Values for Ca and H are assumed to be zero and that for C is a rough estimate derived by comparing the neutron yield curve of C with those for O and Si.

Table 4. Neutron Absorption Cross Section and Rock Composition by Element

Element	Neutron Absorption Cross Section ^a	Rock Composition (ppm) ^b	
		Sandstone	Shale
Li	71.2	15	66
B	761	35	100
O	0.000291	520000	496000
Na	0.532	3300	9600
Mg	0.0666	7000	15000
Al	0.2302	25000	80000
Si	0.1669	368000	273000
Cl	33.63	10	180
K	2.11	10700	26600
Ca	0.432	39100	22100
Ti	6.11	1500	4600
Cr	3.02	35	90
Mn	13.31	100	850
Fe	2.61	9800	47200
Co	37.198	0.3	19
Ni	4.52	2	68
Sm	5610	10	6.4
Eu	4570	1.6	1
Gd	48860	5	3.2

^a*Lide* [2000].

^b*Parker* [1967].

2. Using the isotope abundance ($^{36}\text{Cl}/\text{Cl}$ ratio) to calculate age, a method intended to reduce error associated with varying composition of groundwater at recharge, may yield less accurate results than using ^{36}Cl concentration alone, due to diffusion of dead chloride into the aquifer.

3. Subsurface production of ^{36}Cl by neutron activation within neighboring aquitards, which can then diffuse over a limited distance (perhaps 30 m) into an aquifer, may be a more significant source of the isotope than production within the aquifer itself. This source, which is likely to be significant where fine-grained beds are richer in U and Th and contain more saline groundwater than aquifers, should be considered when estimating the effect of subsurface production on ^{36}Cl age determinations.

4. As a result of diffusive losses and subsurface production, the maximum dateable age by the ^{36}Cl method is considerably less than expected from the isotope's half-life.

5. Where cross-formational flow is significant, trends observed in ^{36}Cl age are not likely to reflect the rates or even direction of flow within an aquifer. The isotope distribution and abundance, on the other hand, may provide clues about the rates and nature (i.e., matrix versus fracture control) of cross-formation flow.

6. Groundwater age cannot be interpreted directly from ^{36}Cl concentration or isotopic abundance where groundwater is even moderately saline. In our simple models the ^{36}Cl concentration failed to predict groundwater age where groundwater chlorinity exceeded ~ 75 – 150 mg kg^{-1} .

7. Long stretches along groundwater flow paths where ^{36}Cl concentration changes little need not be interpreted as containing stagnant water. This condition more likely reflects the need to invoke a method more sophisticated than the piston flow model to describe mass transport.

[56] The calculations further demonstrate the potential of reactive transport modeling applied to interpret the distribution of radioisotopes in groundwater flow regimes and to better estimate

the rates and patterns of groundwater flow from these distributions than is possible with the piston flow model.

Appendix A: Neutron Production Rate

[57] The rate at which ^{36}Cl is produced in situ within basin sediments by neutron activation depends in part on the neutron flux within the medium, which reflects the composition of rock grains. The neutron production rate P_n , in neutrons per gram of rock per year, can be calculated from the U and Th content of rock grains using the correlation [Andrews, 1985]

$$P_n = A_1[\text{U}] + A_2[\text{Th}]. \quad (16)$$

Here, [U] and [Th] are the U and Th contents of the rock, in mg kg^{-1} and A_1 and A_2 (section 3.3) are the number of neutrons produced per micrograms of U and Th per year. Values for these coefficients are given by the relations [Andrews et al., 1989]

$$A_1 = \frac{\sum_i S_i F_i Y_i^U}{\sum_i S_i F_i} + \frac{N_A \lambda_{sf} v_{sf}}{A_{238} \times 10^6} \quad (17)$$

$$A_2 = \frac{\sum_i S_i F_i Y_i^{Th}}{\sum_i S_i F_i}. \quad (18)$$

Here, i serves to index the light elements (we consider C, O, F, Na, Mg, Al, Si, K, and Ca) that emit neutrons when bombarded with alpha particles from U and Th alpha decay chains, S_i is the mass stopping power of each element i (in $\text{MeV g}^{-1} \text{cm}^{-2}$), F_i is the mass fraction of the element in the rock, N_A is Avogadro's number, λ_{sf} is the spontaneous fission rate ($8.5 \times 10^{-17} \text{ yr}^{-1}$ [Andrews et al., 1989]) of ^{238}U , v_{sf} is average number of neutrons per spontaneous fission of ^{238}U (≈ 2.2 [Andrews et al., 1989]), A_{238} is atomic weight (238.03) of U, and Y_i^U and Y_i^{Th} are the neutron yields of the element per μg of U and Th per year. We take values for S_i , F_i , and Y_i from Parker [1967], Feige et al. [1968], and Andrews et al. [1989]. The right-hand term in equation (17) is the number (0.4731) of neutrons produced by spontaneous fission of ^{238}U , per μg of U per year. We take the composition of light elements, which affects the neutron production, as the average composition of sandstone and shale (for the aquifer and aquitards, respectively), from Parker [1967]; see Table 3.

[58] The neutron production rate P_n can be converted to a neutron flux Φ_n (neutrons $\text{cm}^{-2} \text{yr}^{-1}$) according to

$$\Phi_n = \frac{P_n}{\sum_i N_i \sigma_i}, \quad (19)$$

where σ_i is the neutron absorption cross section of element i (in cm^2) and N_i is the number of atoms of the element per gram of rock (as calculated from data in Table 4). The ^{36}Cl production rate is calculated using equation (3).

[59] **Acknowledgments.** We thank Hernán Quinodoz, Theresa Fritzel, and Annette Fugl for their assistance in initiating this study and helping prepare the modeling techniques and software. This material is based on work supported by the National Science Foundation under grant EAR 94-17768. Any opinions, findings, and conclusions or recommendations

expressed in this material are those of the authors and do not necessarily reflect those of the National Science Foundation. Computational resources and software development costs were provided by the research sponsors of the Hydrogeology Program at the University of Illinois: Amoco, ARCO, Chevron, Conoco, Exxon, Hewlett-Packard, Japan National Oil Corp., Lawrence Livermore, Mobil, Sandia, Silicon Graphics, Texaco, and the U.S. Geological Survey.

References

- Andrews, J. N., The isotopic composition of radiogenic helium and its use to study groundwater movement in confined aquifers, *Chem. Geol.*, **49**, 339–351, 1985.
- Andrews, J. N., S. N. Davis, J. T. Fabryka-Martin, J. C. Fontes, B. E. Lehmann, H. H. Loosli, J. L. Michelot, H. Moser, B. Smith, and M. Wolf, The in situ production of radioisotopes in rock matrices with particular reference to the Stripa granite, *Geochim. Cosmochim. Acta*, **53**, 1803–1815, 1989.
- Andrews, J. N., J.-C. Fontes, J.-L. Michelot, and D. Elmore, In-situ neutron flux, ^{36}Cl production and groundwater evolution in crystalline rocks at Stripa, Sweden, *Earth Planet. Sci. Lett.*, **77**, 49–58, 1986.
- Andrews, J. N., T. Florkowski, B. E. Lehmann, and H. H. Loosli, Underground production of radionuclide in the Milk River aquifer, Alberta, Canada, *Appl. Geochem.*, **6**, 425–434, 1991.
- Barone, F. S., R. K. Rowe, and R. M. Quigley, Laboratory determination of chloride diffusion coefficient in an intact shale, *Can. Geotech. J.*, **27**, 177–184, 1990.
- Bentley, H. W., F. M. Phillips, and S. N. Davis, Chlorine-36 in the terrestrial environment, in *Handbook of Environmental Isotope Geochemistry*, edited by P. Fritz and J. C. Fontes, pp. 427–480, Elsevier Sci., New York, 1986a.
- Bentley, H. W., F. M. Phillips, S. N. Davis, M. A. Habermehl, P. L. Airey, G. E. Calf, D. Elmore, H. E. Gove, and T. Torgersen, Chlorine-36 dating of very old groundwater 1. The Great Artesian Basin, Australia, *Water Resour. Res.*, **22**, 1991–2001, 1986b.
- Bethke, C. M., A numerical model of compaction-driven groundwater flow and heat transfer and its application to the paleohydrology of intracratonic sedimentary basin, *J. Geophys. Res.*, **90**, 6817–6828, 1985.
- Bethke, C. M., M. K. Lee, and J. Park, Basin modeling with Basin2 Release 4: A guide to using the Basin2 software package, Hydrogeol. Program, Univ. of Ill., Urbana, 1999a.
- Bethke, C. M., X. Zhao, and T. Torgersen, Groundwater flow and the ^4He distribution in the Great Artesian Basin of Australia, *J. Geophys. Res.*, **104**, 12,999–13,011, 1999b.
- Davis, S. N., L. D. Cecil, M. G. Zreda, and P. Sharma, Chlorine-36 and the initial value problem, *Hydrogeol. J.*, **6**, 104–114, 1998.
- Davis, S. N., J. T. Fabryka-Martin, L. Wolfsberg, S. Moyses, R. Shaver, E. J. Calvin Alexander, and N. Krothe, Chlorine-36 in ground water containing low chloride concentrations, *Ground Water*, **38**, 912–921, 2000.
- Domenico, P. A., and F. W. Schwartz, *Physical and Chemical Hydrogeology*, John Wiley, New York, 1990.
- Etchevery, D., and P. Perrochet, Direct simulation of groundwater transit-time distributions using the reservoir theory, *Hydrogeol. J.*, **8**, 200–208, 2000.
- Faure, G., *Principles of Isotope Geology*, 2nd ed., 589 pp., John Wiley, New York, 1986.
- Feige, Y., B. G. Oltman, and J. Kastner, Production rates of neutrons in soils due to natural radioactivity, *J. Geophys. Res.*, **73**, 3135–3142, 1968.
- Fritzel, T. L. B., Numerical modeling of the distribution of ^3He and ^4He in groundwater flow systems with applications in determining the residence times of very old groundwaters, M.S. thesis, 109 pp., Univ. of Ill., Urbana, 1996.
- Fröhlich, K., M. Ivanovich, M. J. Hendry, J. N. Andrews, S. N. Davis, R. J. Drimmie, J. T. Fabryka-Martin, T. Florkowski, and P. Fritz, Application of isotopic methods to dating of very old groundwaters: Milk River aquifer, Alberta, Canada, *Appl. Geochem.*, **6**, 465–472, 1991.
- Goode, D. J., Direct simulation of groundwater age, *Water Resour. Res.*, **32**, 289–296, 1996.
- Hendry, M. J., and F. W. Schwartz, An alternative view on the origin of chemical and isotopic patterns in groundwater from the Milk River Aquifer, Canada, *Water Resour. Res.*, **24**, 1747–1763, 1988.
- Hendry, M. J., L. I. Wassenaar, and T. Kotzer, Chloride and chlorine isotopes (^{36}Cl and ^{37}Cl) as tracers of solute migration in a thick, clay-rich aquitard system, *Water Resour. Res.*, **36**, 285–296, 2000.
- Lehmann, B. E., S. N. Davis, and J. T. Fabryka-Martin, Atmospheric and subsurface sources of stable and radioactive nuclides used for groundwater dating, *Water Resour. Res.*, **29**, 2027–2040, 1993.

- Lide, D. R., *CRC Handbook of Chemistry and Physics*, 81st ed., CRC Press, Boca Raton, Fla., 2000.
- Love, A. J., A. L. Herczeg, L. Sampson, R. G. Cresswell, and L. K. Fifield, Sources of chloride and implications for ^{36}Cl dating of old groundwater, southwestern Great Artesian Basin, Australia, *Water Resour. Res.*, 36, 1561–1574, 2000.
- Nolte, E., P. Krauthan, G. Korschinek, P. Maloszewski, P. Fritz, and M. Wolf, Measurements and interpretations of ^{36}Cl in groundwater, Milk River aquifer, Alberta, Canada, *Appl. Geochem.*, 6, 435–445, 1991.
- Parker, R. L., Compositions of the Earth's crust, in *Data of Geochemistry*, 6th ed., chap. D, U.S. Geol. Surv., Reston, Va., 1967.
- Phillips, F. M., H. W. Bentley, S. N. Davis, D. Elmore, and G. B. Swanick, Chlorine 36 dating of very old groundwater, 2, Milk River aquifer, Alberta, Canada, *Water Resour. Res.*, 22, 2003–2016, 1986.
- Plummer, M. A., F. M. Phillips, J. T. Fabryka-Martin, H. J. Turin, P. E. Wigand, and P. Sharma, Chlorine-36 in fossil rat urine: An archive of cosmogenic nuclide deposition during the past 40,000 years, *Science*, 277, 538–541, 1997.
- Purdy, C. B., G. R. Helz, A. C. Mignerey, P. W. Kubik, D. Elmore, P. Sharma, and T. Hemmick, Aquia aquifer dissolved Cl^- and $^{36}\text{Cl}/\text{Cl}$: Implications for flow velocities, *Water Resour. Res.*, 32, 1163–1171, 1996.
- Sathaye, J. A., and D. E. Grandstaff, Water rock interaction and the distribution of salinity in the Illinois Basin, *AAPG Bull.*, 80, 1531, 1996.
- Seaman, J. C., P. M. Bertsch, S. F. Korom, and W. P. Miller, Physicochemical controls on nonconservative anion migration in coarse-textured alluvial sediments, *Groundwater*, 34, 778–783, 1996.
- Torgersen, T., M. A. Habermehl, F. M. Phillips, D. Elmore, P. W. Kubik, B. G. Jones, T. Hemmick, and H. E. Gove, Chlorine 36 dating of very old groundwater, 3, Further studies in the Great Artesian Basin, Australia, *Water Resour. Res.*, 27, 3201–3213, 1991.
- Varni, M., and J. Carrera, Simulation of groundwater age distributions, *Water Resour. Res.*, 34, 3271–3281, 1998.
-
- C. M. Bethke, T. M. Johnson, and J. Park, Department of Geology, University of Illinois, 1301 West Green Street, Urbana, IL 61801, USA. (j-park16@students.uiuc.edu)
- T. Torgersen, Department of Marine Science, University of Connecticut, Groton, CT 06340, USA.